Available online at www.sciencedirect.com
SCIENCE DIRECT
Journal of Power Sources 156 (2006) 705–711
JOURNAL OF POWER SOURCES
www.elsevier.com/locate/jpowsour

Analysis of polyaniline-based nickel electrodes for electrochemical supercapacitors

T.C. Girija, M.V. Sangaranarayanan *

Department of Chemistry, Indian Institute of Technology, Chennai 600 036, India

Received 23 February 2005; accepted 17 May 2005
Available online 12 July 2005

Abstract

Polyaniline is deposited potentiodynamically on a nickel substrate in the presence of *p*-toluene sulfonic acid and the specific capacitance is estimated. The electrochemical characterisation of the electrode is carried out by means of cyclic voltammetry, electrochemical impedance spectroscopy, and galvanostatic charge–discharge experiments. The specific capacitance is $\sim 4.05 \times 10^2\,\mathrm{F\,g^{-1}}$. This indicates the feasibility of the polyaniline-coated nickel electrode for use in electrochemical supercapacitors.

Keywords: Polyaniline; Potentiodynamic deposition; Electrochemical supercapacitor; *p*-Toluene sulfonic acid

1. Introduction

Conducting polymers have been studied extensively because of their potential application in sensors and energy-storage devices [1,2]. The polymers can serve as the active electrode materials in rechargeable batteries [3,4], electrochromic devices [5] and electrochemical supercapacitors [6–9]. In recent years, investigations on the design of supercapacitors have increased significantly in view of their enhanced power densities [10]. The materials hitherto studied have essentially been of three types [11], viz., (i) carbon materials of high surface area, (ii) metal oxides such as RuO_2 and MnO_2, (iii) conducting polymers, e.g., polypyrrole and polyaniline. Among these materials, conducting polymers offer the advantages of lower cost in comparison with metal oxides, higher charge densities in contrast to carbon, and satisfactory intrinsic auto-conductivity. Among the conducting polymers, polyaniline (PANI) has attracted much attention because of its environmental stability, controllable electrical conductivity, and easy processability. Electrochemical characterisation studies of PANI electrodes have been reported [12–14] under diverse system parameters. For the practical application of PANI in supercapacitors, it is essential to use inexpensive materials as current-collectors and obtain a large specific capacitance.

Polyaniline is a promising material in the application of electrochemical capacitors, on account of the existence of different oxidation states [1,15]. The redox processes facilitated by the conjugate bond structure are: at potentials negative to 0.20 V, PANI is in an entirely reduced state, designated as leucoemeraldine (LE). At a potential of ~0.20 V, LE undergoes partial oxidation to form the emeraldine (EM) structure. If the potential of PANI becomes more positive, EM undergoes oxidation to yield pernigraniline (PE). The oxidation and reduction processes are accompanied by doping and undoping of counteranions, respectively. Since these processes are reversible, charge storage in PANI is facilitated to yield a pseudocapacitance (C_ϕ) behaviour [16]. Additionally, separation of charges takes place at the PANI electrolyte interface and this gives rise to the existence of a double-layer capacitance (C_{dl}). Thus, the total capacitance, $C_t = C_{dl} + C_\phi$. As these two components depend on the real surface area, it is imperative that PANI-based electrodes should possess a high porosity vis a vis a large specific surface area. Furthermore, the current collector should be inexpensive. In the present

* Corresponding author. Tel.: +91 44 22578269; fax: +91 44 22570545.
E-mail address: mvs@chem.iitm.ac.in (M.V. Sangaranarayanan).

0378-7753/$ – see front matter © 2005 Elsevier B.V. All rights reserved.
doi:10.1016/j.jpowsour.2005.05.051

study, these two favourable aspects – large surface-area and low cost – are achieved by the electrodeposition of PANI on Ni in the presence of *p*-toluene sulfonic acid (PTS).

2. Experimental

Analar grade aniline (SRL Ltd., India) was vacuum-distilled at 120 °C before use, while analar grade PTS (SRL Ltd., India) was used without pretreatment. Double-distilled water was used for the preparation of solutions. Electrochemical measurements were made in a one-compartment cell with a three-electrode configuration. An Ag/AgCl (Bioanalytical systems, USA) was used as the reference electrode, a nickel electrode of 3 mm diameter (Bioanalytical systems, USA) as the working electrode, and platinum foil (Bioanalytical systems, USA) as the counter electrode. Potentials are reported with respect to the Ag/AgCl reference electrode. An electrolyte solution of 0.05 M aniline and 0.5 M PTS was used for electropolymerisation. Deposition of PANI was carried out potentiodynamically by subjecting the working electrode to potential cycling between −0.2 and 1.2 V at a scan rate of 300 mV s^{-1} for 50 cycles. After deposition, the coated polyaniline films were rinsed with 0.5 M PTS in order to remove soluble monomers or oligomeric species.

Cyclic voltammetry, galvanostatic charge–discharge experiments and impedance analysis were performed using an electrochemical workstation CHI 660A (CH Instruments, USA). Impedance measurements were recorded over the frequency range 10^5 to 10^{-3} Hz with an excitation signal of 5 mV. All experiments were conducted at a temperature of 25 ± 1 °C. FT-IR spectra of PTS-doped PANI were obtained with a Perkin-Elmer spectrophotometer. Scanning electrochemical microscopy (SEM) images were recorded using a JEOL JSM-840A instrument. An X-ray diffraction pattern of the sample was obtained with a Shimadzu XD-Dl powder X-ray diffractometer that had a Cu Kα source.

3. Results and discussion

3.1. Infrared spectra

In order to examine the chemical nature, PTS-doped PANI grown on nickel was scraped from the substrate and the IR spectrum was recorded between 2000 and 400 cm^{-1}, see Fig. 1. The origin of the vibrational bands is as follows: at 3280–3400 cm^{-1} due to the NH stretching of aromatic amines, at 2930–3000 cm^{-1} due to aromatic CH-stretching at 556.7 cm^{-1} due to CH out-of-plane bending vibration. The CH out-of-plane bending mode has been used as a key to identifying the type of substituted benzene. The band at 1065.92 cm^{-1} corresponds to the SO^{3-} group of PTS while that at 1114.29 cm^{-1} is due to CH in-plane-bending vibration. The band at 1472.99 cm^{-1} is attributed to CN-stretching of benzenoid rings.

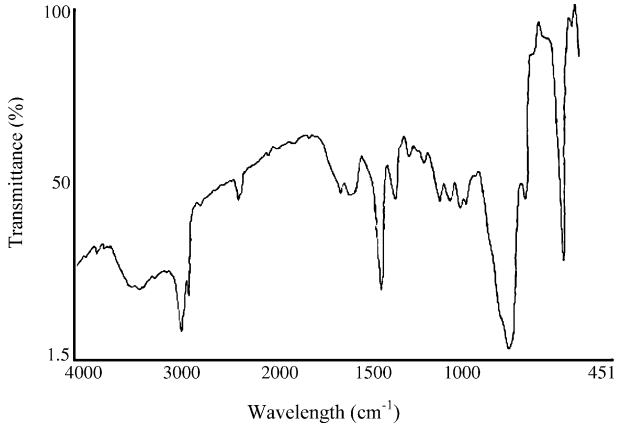

Fig. 1. Infrared spectra of PTS-doped PANI grown by potentiodynamic deposition on nickel substrate.

3.2. SEM characterisation

Scanning electron microscopy (SEM) measurements were carried out in order to deduce the morphology of the electropolymerised PANI which strongly depends on the polymerisation conditions, such as the nature of the solvent, the method of electropolymerisation, etc. A SEM micrograph of the PANI-deposited nickel electrode is shown in Fig. 2. PANI doped with PTS exhibits a spongy and highly porous morphology, which is similar to that reported for PANI grown from acidic aqueous media [17,18] and to that doped with aromatic sulfonic acids. A high porosity of the material is essential in order to obtain high ionic conductivity with a satisfactory power density [19]. PANI particles of the order of ∼70 nm are formed on nickel in the presence of 0.5 M PTS. Such nanostructured PANI materials would be ideal candidates as electrode materials for supercapacitors since they possess the inherent advantage of having high surface-area, which plays a crucial role in increasing the electrochemical activity in comparison with its bulk counterpart.

3.3. XRD results

The XRD pattern of the nickel specimen coated with PTS-doped PANI is presented in Fig. 3. Studies of XRD patterns of PANI are scarce in the literature [20,21]. The XRD pattern of the sample shows reflections at 2θ values of 45 and 52°. By comparison with JPCDF files for nickel compounds, it is found that the above two reflections correspond to either nickel metal or NiO. The latter is present beneath the PANI layer.

3.4. Cyclic voltammetric studies

Voltammograms recorded for 50 continuous cycles during polymerisation of aniline on the nickel substrate in the presence of 0.5 M PTS are given in Fig. 4. A mass loading of 0.013 mg cm^{-2} of PANI on nickel is estimated from the cyclic voltammograms. The anodic and cathodic peaks at

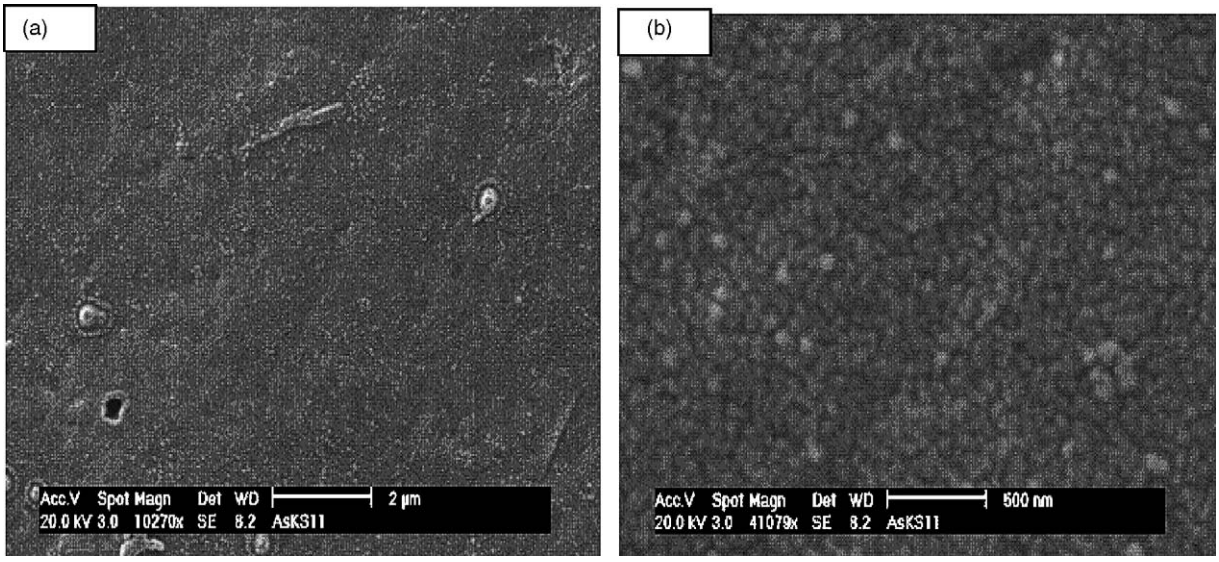

Fig. 2. Scanning electron micrographs of PANI deposited potentiodynamically on nickel foil in presence of 0.5 M PTS at (a) 10270 and (b) 41079× magnification.

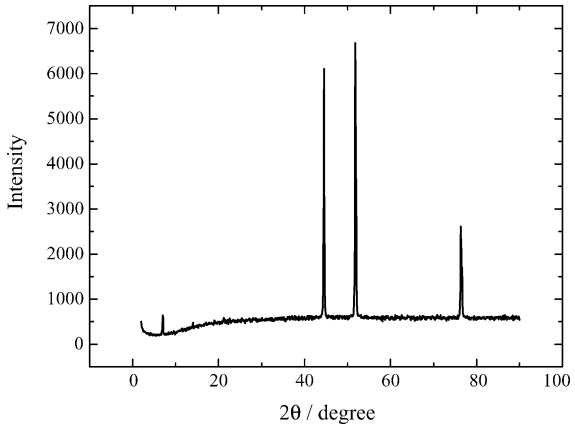

Fig. 3. X-ray diffraction pattern of PTS-doped PANI on nickel. Radiation: Cu Kα.

0.25 and 0.15 V correspond to the LE/EM transition. These peaks shift in positive and negative directions, respectively, as the voltammetric charge increases due to repeated potential scanning. Similarly, the anodic and cathodic peaks at 0.60 and 0.55 V are attributed to the EM/PE transition and also shift with the number of cycles. Cyclic voltammograms for the Ni/ PANI electrode in 0.5 M PTS at different scan rates are shown in Fig. 5. A pseudocapacitive current arising essentially from the redox transitions of the PANI molecular chain is observed and the anodic and cathodic peaks shift in the negative and positive directions, respectively, with increase in scan rate.

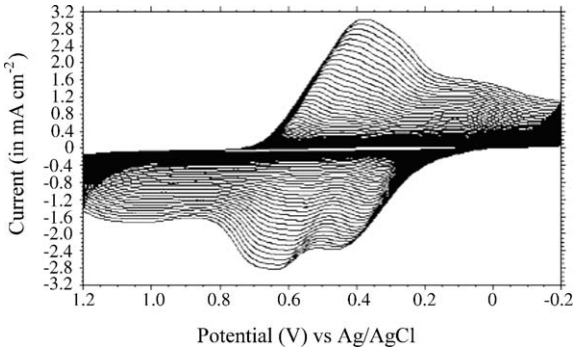

Fig. 4. Multicycle voltammograms depicting electropolymerisation of aniline on nickel from 0.05 M aniline + 0.5 M *p*-toluene sulfonic acid at scan rate of 300 mV s^{-1}.

3.5. Galvanostatic charge–discharge experiments

In order to ascertain the performance of the Ni/PANI electrode material for supercapacitor applications, galvanostatic charge–discharge cycles were analysed for a PANI mass loading of 0.013 mg cm^{-2} on nickel (cf. Fig. 4). A typical chronopotentiogram at a constant current of 1.5 mA cm^{-2} over a potential window of 0.7 V is shown in Fig. 6. This demonstrates the customary charge–discharge behaviour

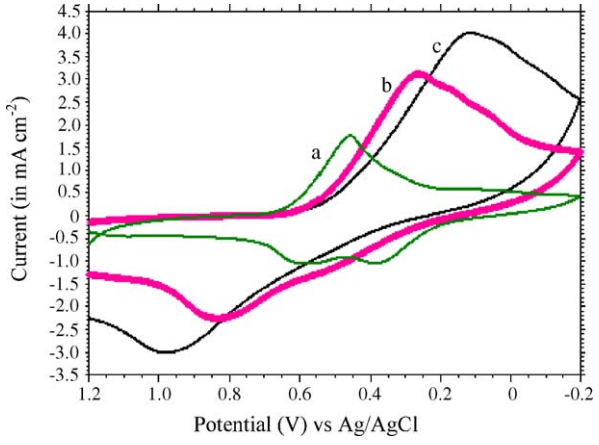

Fig. 5. Cyclic voltammogram for Ni/PANI at various sweep rates: (a) 100 mV s^{-1}, (b) 300 mV s^{-1} and (c) 500 mV s^{-1}.

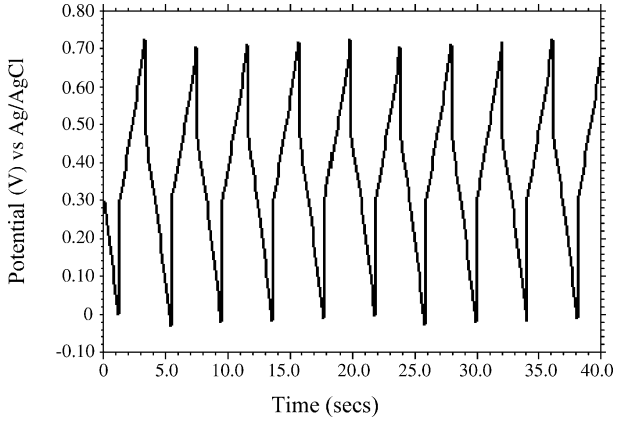

Fig. 6. Galvanostatic charge–discharge curves of Ni/PANI electrode at current density of 1.5 mA cm^{-2}.

(ideally, a ΛΛΛ... shaped voltage response) exhibited by supercapacitors [22]. Furthermore, the charge curves are symmetric to their corresponding discharge counterparts in the potential window and this indicates the feasibility of the Ni/PANI electrode system for the development of supercapacitors. The pseudocapacitance can also be evaluated from charging–discharging responses via chronopotentiometry [23]. The pseudocapacitance is estimated from:

$$C_{cp} = i\Delta t/\Delta v\, m \quad (1)$$

where i, Δt, Δv and m denote, respectively, current density, discharge time, potential range and the active weight of the electrode material. Specific capacitances (in F g^{-1}) of 4.04×10^2, 3.69×10^2, 3.66×10^2 and 3.46×10^2 are obtained at current densities of 0.2, 0.7, 0.9 and 1.5 mA cm^{-2}, respectively. It is inferred that there is no appreciable decrease in capacitance with increase in current density.

In order to evaluate the stability of the electrodes, charge–discharge cycling tests were conducted for 1000 cycles; the performance data are presented in Fig. 7. The specific capacitance of the Ni/PANI electrodes is as high as 346.2 F g^{-1} at an early stage of cycling for 1.5 mA cm^{-2} discharge, but decays to 324.3 F g^{-1} after 1000 cycles. This behaviour is consistent with the performance of other PANI-based electrodes such as PANI/carbon [24], PANI/stainless steel [25] and $LiPF_6$-doped PANI [26].

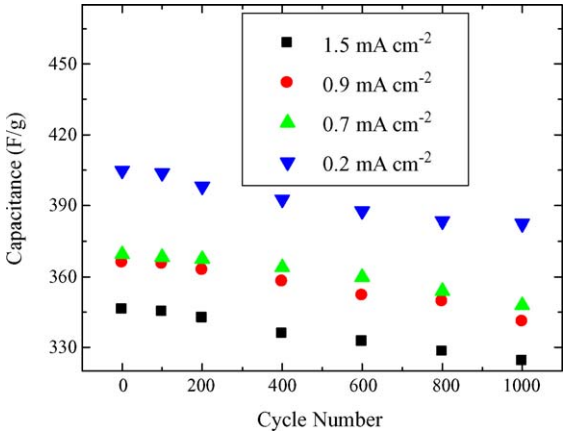

Fig. 7. Variation of capacitance with cycle number at various values of current. PANI mass loading: 0.013 mg cm^{-2}.

3.6. Electrochemical impedance spectroscopy

Electrochemical impedance spectroscopy (EIS) was employed to investigate the mechanistic aspects and the impedance spectra were recorded for PTS-doped PANI/Ni electrodes. Typical Nyquist diagrams for the electrodes in 0.5 M PTS solution at different potentials (0.20–0.75 V) are given in Fig. 8. The impedance curves of all the electrodes show a distorted semi-circle in the high-frequency region due to the porosity of PANI and a vertically linear spike in the low-frequency region. The high-frequency intercept of the semi-circle on the real axis yields the ohmic resistance (R_{sol}), while the diameter provides the charge-transfer resistance (R_{ct}) of the PANI|electrolyte interface. The value of R_{ct} increases with the applied voltage, as noticed from the diameter of the semi-circle. It is known that the conductance of PANI is maximum between the EM and PE states and decreases when PANI transforms to the LE state. The angle made by the low-frequency data on the real axis decreases gradually from ~90 to ~45° on increasing the applied potential from 0.20 to 0.75 V. At 0.75 V, a diffusion-controlled doping and undoping of anions occurs in the electrode, and results in Warburg behaviour. There is a gradual transition from capacitance to Warburg nature between 0.20 and 0.75 V. This trend is in agreement with previous reports of PANI-based capacitor systems in aqueous and non-aqueous media on various substrates [27]. From the frequency (f^*) corresponding to the maximum of the imaginary component ($-Z''$) of the semi-circle, the time constant (τ) is calculated using the expression:

$$\tau = 1/2\pi f^* \quad (2)$$

The value of τ obtained from the data of Fig. 8 are in the range of 0.1–6 ms. Low time constants (of the order of ms) are preferred for electrochemical supercapacitors in order to ensure fast charge–discharge characteristics [10]. The low-frequency differential capacitance can be calculated [27] from the variation of the imaginary component of the impedance with the reciprocal of the frequency ($-Z''$ versus $1/f$). The slope of this plot is equal to $1/2\pi C_t$ and for the potential range between 0.20 and 0.75 V, Z'' versus $1/f$ plots exhibit a linear correlation. The capacitance values (in F g^{-1}) at various applied potentials of 0.20, 0.40 and 0.60 V are 3.71×10^2, 3.59×10^2 and 3.42×10^2 respectively. These values are consistent with those obtained from charge–discharge experiments (see Section 3.5, above).

The equivalent circuit in accordance with the above Nyquist plot is presented in Fig. 9. In this model, the double-layer capacity and the Warburg impedance for semi-infinite linear diffusion are replaced by two constant-phase elements

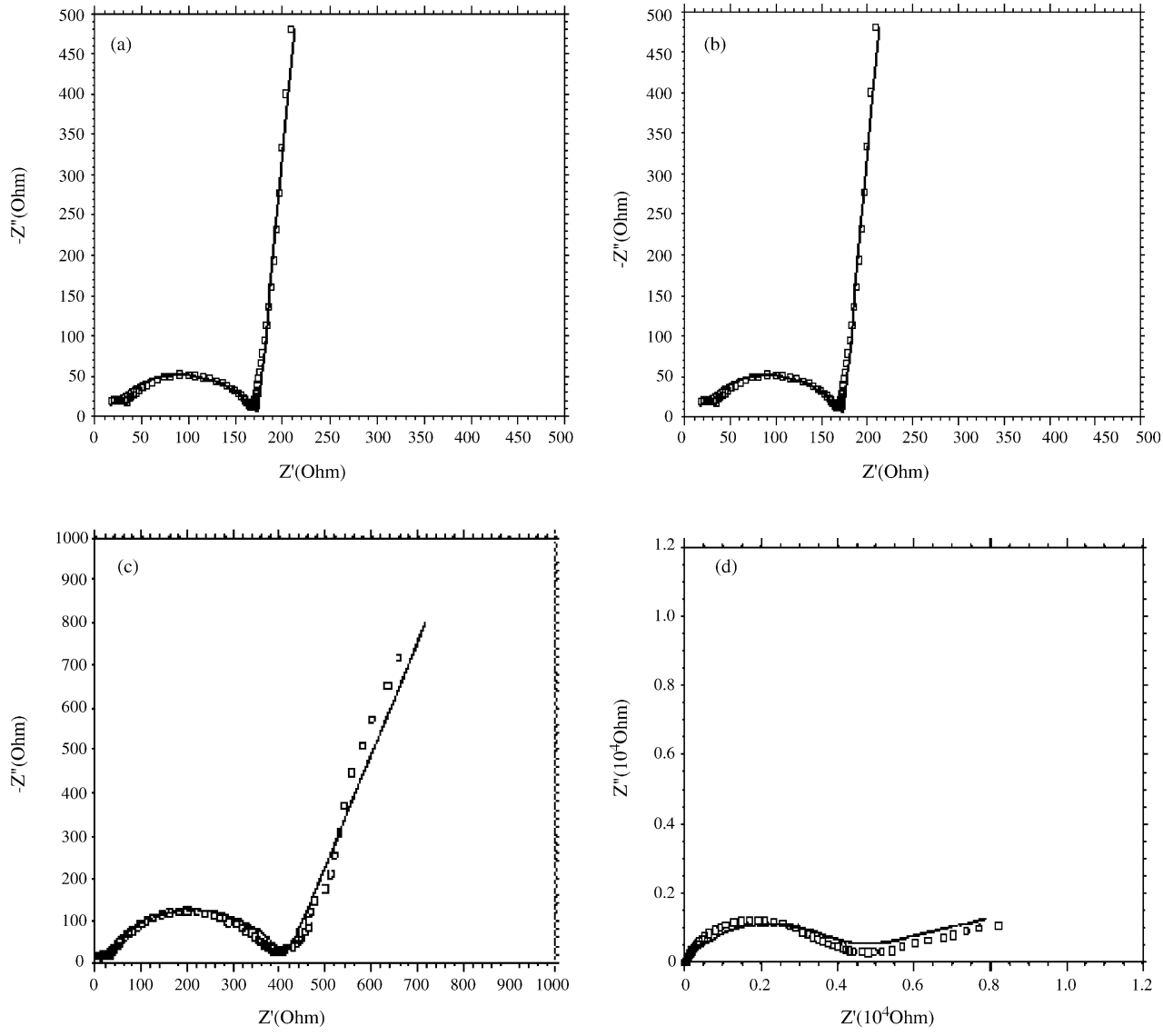

Fig. 8. Impedance spectrum from 10^5 to 10^{-3} Hz of Ni/PANI electrode at various potentials: (a) 0.20 V, (b) 0.40 V, (c) 0.60 V, (d) 0.75 V. Squares denote experimental values while the line represents fitting of data to equivalent circuit of Fig. 8 using parameters in Table 1.

CPE_1 and CPE_2 which correspond, respectively, to a capacity at an inhomogeneous electrode surface and to the diffusion of ions in the electrode. Thus, the double-layer capacity and Warburg impedance of the Randles circuit are replaced by the constant-phase elements. In general, the appearance of a CPE may arise from: (i) a distribution of the relaxation times as a result of inhomogenities existing at the electrode|electrolyte interface; (ii) porosity; (iii) the nature of the electrode; (iv) dynamic disorder associated with diffusion. The proposed equivalent circuit for the PTS-doped PANI electrode can be compared with that of the Ni hexacyanoferrate composite electrode [28] wherein the cations from the electrolyte medium intercalate in and out of the electrode. For the Ni/PANI system, the *p*-toluene sulfonate anions on account of their large size become immobilised in the PANI and a redox process occurs due to the diffusion of the H^+ ions through the polymer material. Hence, incorporation of the two CPE elements in the equivalent circuit that correspond to the porosity of the electrode and the semi-infinite diffusion of the cations becomes necessary. A similar equivalent circuit has also been proposed for indium oxide film electrodes [29]. Fitting of the equivalent circuit was carried out using

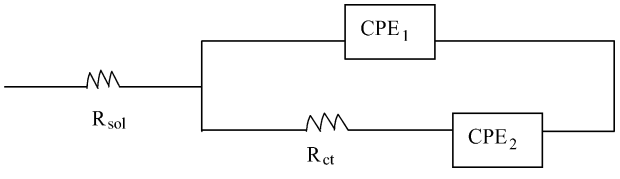

Fig. 9. Equivalent circuit for PTS-doped PANI electrode. R_{sol}-solution resistance, R_{ct}-charge transfer resistance, CPE_1 and CPE_2 denote constant-phase elements.

Table 1
Equivalent circuit parameters deduced by fitting Nyquist plots to circuit of Fig. 9

S. no.	Applied potential (V)	R_{ct} ($\Omega\,cm^2$)	CPE_1 ($\times10^{-5}\,\Omega^{-1}\,cm^{-2}\,s$)	CPE_2 ($\times10^{-3}\,\Omega^{-1}\,cm^{-2}\,s$)	n_1	n_2
1	0.2	165 ± 1	0.8 ± 0.1	8.5 ± 0.5	0.74 ± 0.05	0.95 ± 0.05
2	0.4	348 ± 2	0.7 ± 0.1	7.7 ± 1.0	0.78 ± 0.02	0.90 ± 0.02
3	0.6	408 ± 0.9	1.8 ± 0.05	8.5 ± 0.5	0.70 ± 0.01	0.77 ± 0.05
4	0.75	3500 ± 2	0.084 ± 0.002	0.34 ± 0.05	0.62 ± 0.01	0.18 ± 0.01

the ac impedance simulator of the electrochemical workstation and the parameters of the equivalent circuit are reported in Table 1. The solution resistance R_{sol} is $\sim 8\,\Omega\,cm^2$. The impedances of the two constant-phase elements are defined as [30,31] $Z_{CPE_1} = [Q(j\omega)^{n_1}]^{-1}$ and $Z_{CPE_2} = [Q(j\omega)^{n_2}]^{-1}$ with $-1 \le n \le 1$. The constant value of Q is a combination of properties related to the surface and the electroactive species, while the exponent n arises from the slope of the log Z versus log f plot. The exponent n denotes the correction factor pertaining to the roughness of the electrode and has values that range from 0 to 1. A pure capacitance yields $n = 1$, a pure resistance yields $n = 0$, while $n = 0.5$ represents a Warburg impedance. From the data in Table 1, it follows that in the potential range 0.20–0.60 V (half-oxidised conducting emeraldine state) the value of n_1 deduced as 0.7 refers to the porous nature of the electrode, while the value of n_2 at ~0.9 indicates the highly capacitive nature of the system. At 0.75 V (completely oxidised state) the value of $n_1 = 0.6$ indicates the Warburg behaviour, while $n_2 = 0.2$ implies the resistive nature of the Ni/PANI electrode.

3.7. p-Toluene sulfonic acid doped PANI

From the foregoing analysis, it follows that PTS is an efficient dopant for PANI. During the potentiodynamic deposition of PANI on non-noble metals, the surface oxidation of metals occurs although it does not inhibit nucleation and growth of the PANI [32]. As adsorption of aniline is the primary step for deposition of PANI, it is seen that the adsorption of the monomer takes place on the electrode surface followed by an oxidation step at potentials >0.9 V. Therefore, the surface oxidation of the metal can be prevented if the electrode is passivated with PANI during the initial cycle [32]. In an investigation of PANI deposition on mild steel in the presence of PTS [33], it was observed that PTS allows the surface passivation of the metal without inhibiting the electropolymerisation of aniline. The structure of the *p*-toluene sulfonate anion from which the electrosynthesis of PANI occurs plays a significant role in the surface passivation of non-noble metals: the presence of an aromatic nucleus can limit the oxidation of the metal by blocking its oxidation sites [34]. Hence, PTS is an efficient medium for electrosynthesis of PANI on non-noble metals. When utilised in electrochemical devices [35], sensors [36], etc., the redox processes of conducting polymers at elevated temperatures play a central role since the redox activity is influenced by temperature and the nature of the dopant. It has been reported [37] PTS-doped PANI shows the most stable redox activity at 180 °C due to the thermally stable structure of PTS. Further, while the electrolytes HC1 and H_2SO_4 have low-boiling points and evaporate easily, the conductivity of PANI decreases even below 100 °C. By contrast, PANI doped with organic acids show a stable conductivity [37] up to 150 °C due to the large molecular size of the former and cannot evaporate or exit from the polymer matrix easily. Hence, functionalised organic acids show higher thermal stability than inorganic acids. Although supercapacitors with perchloric acid solutions have been tested [27], these are not desirable as practical devices on account of safety considerations. In this regard, PTS is easy to handle, inexpensive and does not pose any health hazards. It has been demonstrated [38] that the mechanism of the doping process of polymer electrodes can be controlled by varying the nature of the electrolyte used in their electrosynthesis. When electropolymerisation is carried out in the presence of large anions, the anions are immobilised in the polymer structure and consequently the redox process of these modified electrodes must involve the intercalation of cations in and out of the bulk of the electrode. On the other hand, when small anions such as ClO_4^- are employed, the anions themselves are released and act as the mobile-counter species. Since cations diffuse more rapidly than anions, the kinetics of electrodes doped with large anions is faster. It has been inferred [39] that for a large and immobile anion such as *p*-toluene sulfonate, the redox process takes place by the movement of cations inside and outside of the polymer. Therefore, PTS doped PANI electrodes are suitable for improving the response of practical devices in general and capacitors in particular. While the above satisfactory magnitude of capacitance, has been obtained with a three-electrode configuration, for practical capacitors, a two-electrode assembly needs to be constructed, which may reduce the capacitance from the value reported here.

4. Summary

Polyaniline doped with PTS has been deposited potentiodynamically on nickel and its capacitance is estimated. The electrochemical characterisation of these electrodes has been carried out using cyclic voltammetry, electrochemical impedance spectroscopy, and charge–discharge experiments. A specific capacitance of $\sim 4.05 \times 10^2\,F\,g^{-1}$ has been obtained and this value is consistent with those

found from electrochemical impedance spectroscopy and cyclic voltammetry.

Acknowledgements

Financial support by DRDO Government of India is gratefully acknowledged.

References

[1] H.S. Nalwa (Ed.), Handbook of Organic Conductive Molecules and Polymers, vol. 4, Wiley, New York, USA, 1997.
[2] T.A. Skotheim, R.L. Elsenbaumer, J.R. Reynolds (Eds.), Handbook of Conducting Polymers, 2nd ed., Marcel Dekker, New York, 1998.
[3] P. Novak, K. Muller, K.S.V. Santhanam, O. Hass, Chem. Rev. 97 (1997) 207.
[4] Y. Gofer, J.G. Killian, H. Sarker, T.O. Poehler, P.C. Searson, J. Electroanal. Chem. 443 (1998) 103.
[5] A. Bessière, C. Duhamel, J.-C. Badot, V. Lucas, M.-C. Certiat, Electrochim. Acta 49 (2004) 2051.
[6] B.E. Conway, Electrochemical Supercapacitors, Kluwer Academic Publishers/Plenum Press, New York, USA, 1999.
[7] A. Rudge, I. Raistrick, S. Gottesfeld, J.P. Ferraris, Electrochim. Acta 39 (1994) 273.
[8] C. Arbizzani, M. Mastragastino, R. Paraventi, Adv. Mat. 8 (1996) 331.
[9] M.D. Ingram, A.J. Pappin, F. Delalande, D. Poupard, G. Terzouli, Electrochim. Acta 48 (1998) 1601.
[10] A. Burke, J. Power Sources 91 (2000) 37.
[11] S. Sarangapani, B.V. Tilak, C.P. Chen, J. Electrochem. Soc. 143 (1996) 3791.
[12] D. Belanger, X. Ren, J. Davey, F. Uribe, S. Gottesfeld, J. Electrochem. Soc. 147 (2000) 2923.
[13] F. Fusalba, P. Gouerec, D. Villers, D. Belanger, J. Electrochem. Soc. 148 (2001) A1.
[14] K.S. Ryu, K.M. Kim, N.G. Park, Y.J. Park, S.H. Chang, J. Power Sources 103 (2002) 305.
[15] D.E. Stilwell, S.M. Park, J. Electrochem. Soc. 135 (1988) 2491.
[16] B.E. Conway, V. Briss, J. Wojtowicz, J. Power Sources 66 (1997) 1.
[17] T. Osaka, K. Nakajima, K. Shiota, T. Momma, J. Electrochem. Soc. 138 (1992) 2853.
[18] S. Yonezama, K. Kanamura, Z. Takehara, J. Electrochem. Soc. 140 (1993) 629.
[19] B.E. Conway, J. Electrochem. Soc. 138 (1991) 1539.
[20] A.G. MacDiarmid, A.J. Epstein, Science and Applications of Conducting Polymers, Adam Hilger, Bristol, MA, 1991, p. 117.
[21] M.E. Jozefowicz, A.J. Epstein, J.P. Pouget, J.G. Masters, A. Ray, A. Sun, X. Tang, A.G. MacDiarmid, Synth. Met. 41–43 (1991) 723.
[22] Chi-Chang Hu, Chen-Ching Wang, Electrochem. Commun. 4 (2002) 554.
[23] Wei-Chih Chen, Ten-Chin Wen, J. Power Sources 117 (2003) 273.
[24] Wei-Chih Chen, Ten-Chin Wen, Hsisheng Teng, Electrochim. Acta 48 (2003) 641.
[25] K. RajendraPrasad, N. Munichandraiah, J. Power Sources 112 (2002) 443.
[26] K.S. Ryu, K.M. Kim, Y.J. Park, N.-G. Park, M.G. Kang, S.H. Chang, Solid State Ionics 152/153 (2002) 861.
[27] D. Belanger, X. Ren, J. Davey, F. Uribe, S. Gottesdeld, J. Electrochem. Soc. 147 (2000) 2923, and references therein.
[28] U. Retter, A. Widmann, K. Siegler, H. Kahlert, J. Electroanal. Chem. 546 (2003) 87.
[29] M. Metikos-Hukovic, S. Omanovic, J. Electroanal. Chem. 455 (1998) 181.
[30] J.O. Agak, R. Stoodley, U. Retter, D. Bizzotto, J. Electroanal. Chem. 562 (2004) 35.
[31] U. Retter, H. Lozhse, in: F. Scholz (Ed.), Electroanalytical Methods, Springer, 2002.
[32] K. RajendraPrasad, N. Munichandraiah, Synth. Met. 123 (2001) 459.
[33] J.L. Camalet, J.C. Lacroix, S. Aeiyach, P.C. Lacaze, J. Electroanal. Chem. 445 (1998) 117.
[34] J.J. Kester, J.E. Furtak, A.J. Bevuly, J. Electrochem. Soc. 129 (1982) 716.
[35] A.G. MacDiarmid, L.S. Yang, Synth. Met. 13 (1986) 193.
[36] E. Wang, A. Liv, Anal. Chim. Acta 252 (1991) 53.
[37] S. Kim, I.J. Chung, Synth. Met. 97 (1998) 127.
[38] V.D. Pokhodenko, V.A. Krylov, Synth. Met. 41 (1991) 533.
[39] J.R. Reynolds, M. Pyo, Y.-J. Qiu, Synth. Met. 55–57 (1993) 1388.